PERK mediates eIF2α phosphorylation responsible for BACE1 elevation, CREB dysfunction and neurodegeneration in a mouse model of Alzheimer's disease

Latha Devi[a] and **Masuo Ohno**[a,b,*]

[a]Center for Dementia Research, Nathan Kline Institute, Orangeburg, NY, USA

[b]Department of Psychiatry, New York University Langone Medical Center, New York, NY, USA

Abstract

Emerging evidence suggests that aberrant phosphorylation of eukaryotic initiation factor-2α (eIF2α) may induce synaptic failure and neurodegeneration through persistent translational inhibition of global protein synthesis. However, elevated phospho-eIF2α also paradoxically causes translational activation of a subset of mRNAs such as the β-secretase enzyme BACE1 and CREB repressor ATF4. Therefore, we tested whether genetic reduction of the eIF2α kinase PERK may prevent these deleterious events and mitigate Alzheimer's disease (AD)-like neuropathology and cognitive impairments in the 5XFAD mouse model. PERK haploinsufficiency blocked overactivation of the PERK-eIF2α pathway, as evidenced by significant reductions in phosphorylation of PERK and eIF2α, in 5XFAD mice. PERK haploinsufficiency was sufficient to rescue memory deficits and cholinergic neurodegeneration in this AD model. Notably, PERK haploinsufficiency also prevented BACE1 elevations, resulting in reduced levels of amyloid-β peptides and plaque burden in 5XFAD mice. Moreover, CREB dysfunction was restored in PERK$^{+/-}$·5XFAD mice concomitant with reversal of ATF4 upregulation. Together, these findings suggest that PERK may be a disease-modifying therapeutic target to prevent multiple memory-disrupting mechanisms associated with AD.

Keywords

PERK; eIF2α; BACE1; amyloid-β; ATF4; CREB; cholinergic neuron; fear conditioning; learning and memory; 5XFAD

1. Introduction

Neurodegenerative diseases such as Alzheimer's disease (AD), Parkinson's disease and prion disease are associated with the accumulation of disease-specific misfolded proteins in

*Corresponding author at: Center for Dementia Research, Nathan Kline Institute, 140 Old Orangeburg Road, Orangeburg, NY 10962, USA. Tel.: 845-398-6599; Fax: 845-398-5422; mohno@nki.rfmh.org.

the brain. The presence of misfolded proteins in the endoplasmic reticulum (ER) triggers the unfolded protein response (UPR), a protective cellular mechanism that induces the transient shutdown of protein synthesis through phosphorylation of eukaryotic initiation factor-2α (eIF2α). However, a recent study indicates that sustained translational repression of global protein synthesis resulting from overactivation of the eIF2α phosphorylation pathway may lead to neurodegeneration and synaptic failure in a prion-diseased mouse model (Moreno et al., 2012). Remarkably, protein kinase RNA-like ER kinase (PERK), an eIF2α kinase, has been shown to play a key role in mediating persistently high levels of eIF2α phosphorylation following exposure to misfolded proteins. For example, a specific inhibitor of PERK prevents UPR-mediated translational repression, neurodegeneration and clinical signs of prion disease in prion-infected mice (Moreno et al., 2013). Similarly, genetic deletion of PERK not only in amyloid precursor protein (APP) transgenic mice but also in amyloid-β (Aβ)-treated hippocampal slices reverses eIF2α phosphorylation-dependent inhibition of general protein synthesis and rescues deficits in CA1 synaptic plasticity and memory function (Ma et al., 2013). Both investigations reveal that pharmacologic or genetic suppression of PERK restores UPR overactivation-associated reductions in synthesis of vital synaptic proteins, suggesting that PERK may be a critical therapeutic target downstream to accumulation of misfolded prion protein or Aβ in these neurodegenerative diseases.

Whereas phosphorylation of eIF2α at Ser51 inhibits general translation initiation, it is known to paradoxically cause translational activation of a subset of mRNAs that contain upstream open reading frames. These include the β-secretase called β-site APP-cleaving enzyme 1 (BACE1) (De Pietri Tonelli et al., 2004; Devi and Ohno, 2010b; Lammich et al., 2004; Mihailovich et al., 2007; O'Connor et al., 2008) and the transcriptional modulator activating transcription factor 4 (ATF4) (Harding et al., 2000a; Vattem and Wek, 2004). In fact, protein levels of BACE1, a key enzyme responsible for initiating Aβ production, are significantly elevated (Cai et al., 2012; Fukumoto et al., 2002; Holsinger et al., 2002; Li et al., 2004; Ohno et al., 2007; Yang et al., 2003; Zhao et al., 2007) concomitant with increased levels of phosphorylated eIF2α in brains of AD patients and different lines of APP transgenic mice (Chang et al., 2002; Devi and Ohno, 2010b; Devi and Ohno, 2013b; Kim et al., 2007; Mouton-Liger et al., 2012; O'Connor et al., 2008; Page et al., 2006). Furthermore, a recent report demonstrates AD-related upregulation of ATF4 (Lewerenz and Maher, 2009), which works as a repressor of cAMP response element binding protein (CREB)-dependent transcription responsible for memory consolidation (CREB2) (Chen et al., 2003; Silva et al., 1998). These findings suggest that the overactivated eIF2α phosphorylation pathway may contribute to AD pathogenesis and cognitive impairments not only by inhibiting global protein synthesis but also by accelerating β-amyloidogenesis through BACE1 elevations and directly suppressing CREB function. However, the causative signaling mechanisms remain unclear. In this study, we examined whether PERK haploinsufficiency could block deleterious BACE1/ATF4-elevating pathways and consequently lead to therapeutic benefits including memory improvements in a mouse model of AD.

2. Methods

2.1. Subjects

We used 5XFAD mice (Tg6799 line) that co-overexpress familial AD (FAD) mutant forms of human APP (the Swedish mutation: K670N, M671L; the Florida mutation: I716V; the London mutation: V717I) and presenilin 1 (PS1) (M146L and L286V mutations) transgenes under transcriptional control of the neuron-specific Thy-1 promoter (Oakley et al., 2006; Ohno et al., 2006; Ohno et al., 2007). Although PERK mice show growth retardation, inability to breed and early mortality, the heterozygotes are viable and fertile with normal weight and longevity (Harding et al., 2001; Zhang et al., 2002). Therefore, hemizygous 5XFAD transgenic mice (C57BL/6 background) were crossbred to heterozygous PERK knockout mice (C57BL/6 background) (Harding et al., 2000b), yielding animals with four different genotypes (wild-type, PERK$^{+/-}$, 5XFAD$^{+/-}$, and PERK$^{+/-}$·5XFAD$^{+/-}$). Genotyping was performed by PCR analysis of tail DNA and all experiments were done blind with respect to the genotype of mice. In this study, we investigated the effects of PERK haploinsufficiency in 5XFAD mice at 8–9 months of age, which exhibit significant elevations in BACE1 and ATF4 expression (Devi and Ohno, 2010a; Devi and Ohno, 2013a; Zhao et al., 2007). Since our previous study shows that there is no sex difference in cerebral Aβ levels in 5XFAD mice except for the younger age (3 months) (Oakley et al., 2006), a similar number of males and females were used for the experiments. All animal procedures were approved by the Nathan Kline Institute Animal Care and Use Committee and conducted in accordance with the National Institutes of Health Guide for the Care and Use of Laboratory Animals.

2.2. Contextual fear conditioning

Contextual fear conditioning was tested as described previously (Kimura et al., 2010; Kimura and Ohno, 2009; Ohno et al., 2001). In this behavioral assay, mice learn to associate a distinct context (CS: conditioned stimulus) with aversive footshocks (US: unconditioned stimulus) through hippocampus-dependent mechanisms (Fanselow, 2000; Maren, 2001). During training, mice were placed in the conditioning chamber for 3 min and then received two footshocks (1.0 mA, 2 s) at a 1-min interval. After the last shock delivery, mice were left in the chamber for another 30 s. Contextual fear memory was evaluated by scoring freezing behavior (the absence of all movement except for that needed for breathing) for 3 min when the mice were placed back into the same conditioning chamber 24 h after training. The automated FreezeFrame system (Coulbourn Instruments, Allentown, PA, USA) was used to score the amount of freezing during training and memory test sessions. After behavioral testing, some mice were sacrificed for immunoblotting/ELISA experiments and others were perfused for immunohistochemistry.

2.3. Immunoblot analysis

Hippocampal samples were taken from the mice under deep isoflurane anesthesia and were snap-frozen for biochemical assays. For western blot analysis, each sample was homogenized in 5 volumes of modified RIPA buffer containing 150 mM NaCl, 50 mM Tris HCl (pH 8.0), 1 mM EDTA, 1% IGEPAL, 0.5% sodium deoxycholate, 0.1% SDS and protease/phosphatase inhibitor cocktail (Calbiochem, La Jolla, CA, USA), and centrifuged at

10,000 g for 10 min to remove any insoluble material. Protein concentrations were determined by a BCA protein assay kit (Pierce, Rockford, IL, USA), and 10–50 μg of protein was run on NuPAGE 4–12% Bis-Tris gels or 7% Tris-Acetate gels (Invitrogen, Carlsbad, CA, USA) and transferred to nitrocellulose membrane. After blocking, membranes were probed with the following primary antibodies: anti-phospho-PERK (Ser713) (1:1,000, #649401, BioLegend, San Diego, CA), anti-phospho-eIF2α (Ser51) (1:1,000, #3398, Cell Signaling Technology, Danvers, MA, USA), anti-eIF2α (1:2,000, #9722, Cell Signaling Technology), anti-BACE1 (1:1,000, B0681, Sigma-Aldrich, St. Louis, MO, USA), an antibody that recognizes C-terminal epitope in APP (1:1,000, C1/6.1, kindly provided by Dr. Paul Mathews, Nathan Kline Institute) to detect full-length APP/C-terminal fragments, anti-neprilysin (1:1,000, ab951, Abcam, Cambridge, MA, USA), anti-ATF4 (1:2,000, 10835-1-AP, Proteintech, Chicago, IL, USA), anti-phospho-CREB (Ser133) (1:1,000, #9198, Cell Signaling Technology), anti-CREB 1:2,000, #9197, Cell Signaling Technology) and anti-β-actin (1:15,000, AC-15, Sigma-Aldrich). They were then incubated with horseradish peroxidase-conjugated secondary IgG. Immunoblot signals were visualized by an ECL chemiluminescence substrate reagent kit (Pierce), and were quantified by densitometric scanning and image analysis using Quantity One software (Bio-Rad Laboratories, Hercules, CA, USA).

2.4. ELISAs of Aβ40 and Aβ42

Sandwich Aβ ELISAs were performed as described previously (Devi and Ohno, 2010b; Devi and Ohno, 2012; Kimura et al., 2010). Briefly, each hippocampal sample was extracted in 8X cold 5 M guanidine HCl plus 50 mM Tris HCl (pH 8.0) buffer, and centrifuged at 20,000 g for 1 h at 4°C to remove insoluble material. Final guanidine HCl concentrations were below 0.1 M. Protein concentrations were determined by a BCA kit (Pierce). To quantitate total levels of cerebral Aβ40 and Aβ42, supernatant fractions were analyzed by a well-established human Aβ40 and Aβ42 ELISA kits (KHB3481 and KHB3441, Invitrogen), respectively, according to the protocol of the manufacturer. Optical densities at 450 nm of each well were read on a VersaMax tunable microplate reader (Molecular Devices, Sunnyvale, CA, USA), and sample Aβ40 and Aβ42 concentrations were determined by comparison with the respective standard curves. Aβ40 and Aβ42 concentration values were normalized to total protein concentrations and expressed as the percentage of 5XFAD mouse controls.

2.5. Aβ immunohistochemistry

Mice were transcardially perfused with 0.1 M phosphate buffered saline (PBS, pH7.4), followed by 4% paraformaldehyde in PBS under deep isoflurane anesthesia. Brains were postfixed for 24 h in 4% paraformaldehyde in PBS at 4°C and transferred to PBS. The brain was sectioned coronally at 30 μm using a vibratome (VT1200, Leica Microsystems, Wetzlar, Germany), and successive sections were stored in PBS containing 0.05% sodium azide at 4°C. Two sections per mouse taken at levels between −1.7 and −1.9 mm to bregma according to the mouse brain atlas of (Franklin and Paxinos, 2008) were stained by the avidin-biotin peroxidase complex (ABC) method as described previously (Devi et al., 2010; Devi and Ohno, 2010a; Kimura et al., 2010). Briefly, the sections were incubated overnight at 4°C with mouse monoclonal anti-Aβ1–16 (6E10) antibody (1:200, SIG-39347; Covance,

Princeton, NJ, USA). The ABC kit (PK-2200; Vector Laboratories, Burlingame, CA, USA) was utilized with 3,3′-diaminobenzidine tetrahydrochloride (DAB) as a chromogen to visualize the reaction product. The sections were then mounted on charged slides, dehydrated in a series of alcohol, cleared in xylene and covered with a coverslip. Light microscopy was conducted on an Axioskop 2 microscope equipped with an AxioCaM HRc digital camera (Zeiss, Oberkochen, Germany) for capturing images. Semi-quantitative analysis was performed using AxioVision imaging software with the AutoMeasure module (Zeiss). The threshold optical density that discriminated staining from background was determined and held constant for all quantifications. Identified objects were individually inspected by the same investigator to confirm the object as a plaque or not in a blinded manner. Percentage area occupied by Aβ deposits in the hippocampus and cortex was assessed bilaterally to compare plaque burden between 5XFAD control and PERK$^{+/-}$·5XFAD mice.

2.6. ChAT immunohistochemistry

Three brain sections per mouse were stained by the ABC method for immunohistochemical analysis of ChAT-positive neurons in the Ch1/2 comprising the medial septum and the vertical limb of the diagonal band, as described (Devi and Ohno, 2010b). The sections were taken at levels between +1.2 and +0.8 mm to bregma according to the atlas of (Franklin and Paxinos, 2008) and incubated overnight at 4°C with polyclonal goat anti-ChAT antibody (1:200; AB144P, Millipore, Billerica, MA, USA). The DAB staining was performed using the ABC kit (PK-6105, Vector Laboratories). After identified objects, following thresholding under an Axioskop 2 microscope (Zeiss), were individually inspected in a blinded manner to confirm the object as a neuron or not, the number of ChAT-positive neurons in the Ch1/2 was counted using AxioVision imaging software (Zeiss). The average of ChAT-positive neuron number per section from each mouse was used to calculate group medians.

2.7. Data analysis

Significant differences between the groups were determined by a one-way ANOVA and *post-hoc* Fisher's PLSD tests were applied following all ANOVAs showing significance. Data were presented as mean ± SEM and the level of significance was set for *p* value less than 0.05.

3. Results

3.1. PERK haploinsufficiency reduces eIF2α phosphorylation in 5XFAD mice

According to accelerated Aβ42 production due to a combination of five FAD mutations, 5XFAD mice begin to develop visible amyloid deposition as early as 2 months of age and exhibit memory declines on hippocampus-dependent behavioral tasks between 4 and 6 months concomitant with moderate Aβ accumulation and impaired synaptic physiology at Schaffer collateral-CA1 pathways (Chen et al., 2012α; Jawhar et al., 2012; Kimura and Ohno, 2009; Oakley et al., 2006; Ohno, 2009; Ohno et al., 2006). As aberrant phosphorylation of eIF2α is observed in AD brains (Chang et al., 2002; Kim et al., 2007; Mouton-Liger et al., 2012; O'Connor et al., 2008), immunoblot analysis of hippocampal

samples showed robust increases in levels of phosphorylated eIF2α in 5XFAD mice at 8–9 months of age ($p < 0.05$) (Fig. 1A, B). This was accompanied by activation of the PERK pathway, as measured by an increase in phosphorylated PERK ($p < 0.05$) in the absence of change in total PERK, in 5XFAD mice. To examine the role of PERK pathway, we crossbred 5XFAD mice with heterozygous PERK knockout mice. First, PERK heterozygosity was confirmed by significant reductions in PERK protein levels in PERK^{+/−} mice ($p < 0.05$) and PERK^{+/−}·5XFAD mice ($p < 0.05$) as compared with respective PERK^{+/+} controls (Fig. 1B, D). Importantly, PERK haploinsufficiency significantly suppressed increases in phosphorylated forms of eIF2α and PERK in 5XFAD mice ($p < 0.05$) without affecting total eIF2α levels, suggesting that PERK is a major eIF2α kinase responsible for mediating robust eIF2α phosphorylation in this mouse model. In contrast, PERK^{+/−} mice showed no change in phosphorylated eIF2α as compared with wild-type controls, although they had reduced levels of PERK phosphorylation ($p < 0.05$) (Fig. 1C, D). Therefore, PERK seems to be specifically involved in overactivating the eIF2α phosphorylation pathway under AD conditions.

3.2. PERK haploinsufficiency rescues memory deficits and cholinergic neurodegeneration in 5XFAD mice

To test whether suppressing PERK-dependent phosphorylation of eIF2α can rescue memory deficits in 5XFAD mice, we used the hippocampus-dependent contextual fear conditioning paradigm (Fig. 2A). Wild-type control mice exhibited a robust conditioned fear response as assessed by freezing (the absence of all but respiratory movements) when placed back into the conditioning chamber 24 h after training with two CS-US pairings. 5XFAD mice showed significantly reduced levels of freezing compared with wild-type controls ($p < 0.05$), whereas the contextual memory impairment was rescued almost completely back to wild-type levels in PERK^{+/−}·5XFAD mice ($p < 0.05$). Furthermore, freezing levels were indistinguishable between PERK^{+/−} and wild-type mice, indicating that PERK haploinsufficiency does not affect baseline memory performances on the wild-type background.

Freezing behavior was also measured during training (Fig. 2B). While basal levels of freezing before the first footshock were not different between the four groups of mice tested, post-shock freezing was significantly increased in 5XFAD mice irrespective of the presence of PERK mutation ($p < 0.05$). This implies that 5XFAD mice may have even greater abilities to associate the context with aversive shocks, resulting in the higher expression of fear response during training. Nevertheless, 5XFAD mice exhibited deficient contextual memory, which was shown by significantly lower levels of freezing in 24-h retention test as compared with wild-type controls (Fig. 2A). Importantly, post-shock freezing levels were equivalent between 5XFAD and PERK^{+/−}·5XFAD mice, suggesting that the change in the expression of freezing is not likely to account for memory improvements associated with PERK haploinsufficiency in 5XAFD mice.

The septohippocampal cholinergic pathway has an established role in memory performances including the contextual fear conditioning (Gale et al., 2001), while cholinergic neuron loss is found in several AD transgenic mouse models such as 5XFAD and APP23 (Choi et al.,

2013; Devi and Ohno, 2010b). In order to determine whether PERK haploinsufficiency can rescue neurodegeneration concomitant with mnemonic improvements, we analyzed cholinergic neurons in the medial septum and the vertical limb of the diagonal band (Ch1/2) that provide the cholinergic innervation to the hippocampus (Fig. 2C). Immunostaining for choline acetyltransferase (ChAT: a cholinergic marker) revealed that the number of cholinergic neurons was significantly reduced in 5XFAD mice as compared with that of wild-type controls ($p < 0.05$) (Fig. 2D). Remarkably, ChAT-positive neuron number in PERK$^{+/-}$·5XFAD mice was significantly higher than that of 5XFAD mice ($p < 0.05$) and nearly equivalent to wild-type control levels. Therefore, overactivated PERK-dependent eIF2α phosphorylation may be an important mediator of cholinergic neuron death associated with AD.

3.3. PERK haploinsufficiency mitigates β-amyloidosis in 5XFAD mice

In accordance with recent data from our laboratory and others (Devi and Ohno, 2010b; Devi and Ohno, 2013b; Mouton-Liger et al., 2012; O'Connor et al., 2008), the robust increase in eIF2α phosphorylation was closely associated with BACE1 elevation in 5XFAD mice (Fig. 3A, B). We found that suppression of eIF2α phosphorylation in PERK$^{+/-}$·5XFAD mice almost completely reversed their BACE1 expression to wild-type control levels ($p < 0.05$), demonstrating that the PERK-dependent eIF2α phosphorylation pathway mediates BACE1 elevation in this mouse model. Interestingly, PERK haploinsufficiency also partially but significantly reduced expression of full-length APP in 5XFAD mice ($p < 0.05$). Consistent with these changes, levels of the β-cleaved C-terminal fragment of APP (C99) in PERK$^{+/-}$·5XFAD mice were dramatically lower than those of 5XFAD mice ($p < 0.05$). Therefore, PERK haploinsufficiency mitigated Aβ-overproducing mechanisms found in 5XFAD mice. Meanwhile, in agreement with no change in phosphorylated eIF2α levels (Fig. 1C, D), PERK haploinsufficiency on the wild-type background did not affect BACE1 (wild-type, $100 \pm 4.6\%$, $n = 5$; PERK$^{+/-}$, $114.8 \pm 7.2\%$, $n = 5$) or APP (wild-type, $100 \pm 4.8\%$, $n = 5$; PERK$^{+/-}$, $103.6 \pm 5.5\%$, $n = 5$) expression.

Given that net Aβ concentrations in brain are determined by the rate of Aβ generation relative to the overall rate of Aβ clearance, we next examined a possibility that PERK haploinsufficiency may affect Aβ clearance in 5XFAD mice. As observed in human AD brains (Wang et al., 2010), 5XFAD mice showed reductions in the major Aβ-degrading enzyme neprilysin (Fig. 3A, C). Reduced expression of neprilysin was restored in PERK$^{+/-}$·5XFAD mice ($p < 0.05$), suggesting that PERK haploinsufficiency may also correct compromised Aβ clearance in addition to suppressing the β-amyloidogenic processing of APP.

Sandwich ELISAs showed that PERK haploinsufficiency significantly reduced hippocampal Aβ42 levels in 5XFAD mice ($p < 0.05$), while a trend toward reduction of Aβ40 was observed in PERK$^{+/-}$·5XFAD mice compared to 5XFAD mice ($p = 0.08$) (Fig. 3D). In accordance with ELISA data, Aβ immunostaining with 6E10 antibody revealed that hippocampal and cortical plaque loads in PERK$^{+/-}$·5XFAD mice were significantly lower than those in 5XFAD control mice ($p < 0.05$) (Fig. 3E, F). Therefore, genetic suppression of

PERK-dependent eIF2α phosphorylation significantly lowered Aβ accumulation not only through reducing Aβ production but also through facilitating Aβ degradation.

3.4. PERK haploinsufficiency rescues CREB dysfunction in 5XFAD mice

Since eIF2α phosphorylation is also known to induce translational elevation of the CREB repressor ATF4 in addition to BACE1 (Harding et al., 2000a; Vattem and Wek, 2004), we performed immunoblot analysis of hippocampal samples to determine whether PERK haploinsufficiency may affect ATF4 expression and CREB signaling in 5XFAD mice (Fig. 4A). Consistent with changes in phosphorylated eIF2α levels (Fig. 1A, B), ATF4 was significantly increased in 5XFAD mice ($p < 0.05$) while it was reduced to almost wild-type control levels in PERK$^{+/-}$·5XFAD mice ($p < 0.05$) (Fig. 4B). Moreover, PERK haploinsufficiency restored reductions of phosphorylated CREB without affecting total CREB levels in 5XFAD mice ($p < 0.05$). Together, the results suggest that suppressing PERK-mediated eIF2α phosphorylation also reverses ATF4-dependent CREB dysfunction in 5XFAD mice.

4. Discussion

The current study was designed to determine the mechanisms by which aberrant translational machinery through overactivated eIF2α phosphorylation pathways may contribute to the pathogenesis of AD and related memory deficits. The phosphorylation of eIF2α at Ser51 is controlled by four protein kinases such as PERK, double-stranded RNA-activated protein kinase (PKR), general control nonderepressible-2 kinase (GCN2) and heme-regulated inhibitor kinase (HRI) (Costa-Mattioli and Sonenberg, 2008; Donnelly et al., 2013). These eIF2α kinases share a conserved kinase domain but have divergent regulatory domains to specifically become active (i.e., phosphorylated) in response to a variety of cellular stress stimuli. By crossing heterozygous PERK knockout mice with 5XFAD mice, we demonstrate that partial reduction of PERK signaling lowers increased amounts of phosphorylated eIF2α in the hippocampus of this mouse model. Therefore, the PERK pathway accounts for eIF2α phosphorylation that overly occurs with relevance to AD. In contrast, PERK haploinsufficiency is not sufficient to affect basal levels of eIF2α phosphorylation on the wild-type background. It is important to note that homozygous PERK gene knockout that is restricted to the forebrain (Trinh et al., 2012) or complete GCN2$^{-/-}$ ablation (Costa-Mattioli et al., 2005; Devi and Ohno, 2013a) can produce a significant reduction of eIF2α phosphorylation. Together, the greater sensitivity of eIF2α phosphorylation to partial PERK reduction in 5XFAD mice suggests that PERK signaling pathway may play a more prominent role in causing overactivation of eIF2α phosphorylation under exposure to Aβ accumulation rather than in regulating baseline levels of eIF2α phosphorylation under normal physiological conditions.

Importantly, we found that reduced PERK-dependent eIF2α phosphorylation in PERK$^{+/-}$·5XFAD mice leads to amelioration of memory deficits, as tested by the hippocampus-dependent contextual fear conditioning. This is consistent with a recent study showing that forebrain-specific conditional deletion of PERK prevents hippocampal eIF2α phosphorylation and memory impairments in APP/PS1 transgenic mice, as assessed by the hippocampus-dependent spatial learning paradigms such as Morris water maze, Y-water

maze and object location tasks (Ma et al., 2013). Interestingly, this report also reveals that conditional PERK removal can ameliorate deficits in long-term potentiation (LTP: a synaptic plasticity model for learning and memory) at Schaffer collateral-CA1 synapses in Aβ-applied hippocampal slices as well as in APP/PS1 mice. Moreover, global protein synthesis is suppressed concomitant with increased levels of phosphorylated eIF2α in the *in vitro* and *in vivo* AD models, whereas PERK ablation prevents reductions in general protein synthesis and key plasticity-related synaptic proteins as well (Ma et al., 2013). Therefore, two independent investigations using different AD mouse models combined with PERK gene targeting approaches consistently suggest that overactivation of the PERK-dependent eIF2α phosphorylation pathway may cause memory deficits associated with AD, at least in part, through translational suppression of general protein synthesis as a downstream branch of excess Aβ accumulation.

As opposed to the general protein synthesis inhibition, it has been indicated that eIF2α phosphorylation paradoxically induces translational upregulation of the β-secretase enzyme BACE1 (Devi and Ohno, 2010b; Mouton-Liger et al., 2012; O'Connor et al., 2008). We previously reported that 6-month-old 5XFAD mice, which have not yet showed BACE1 upregulation, have only marginal changes in eIF2α phosphorylation, whereas levels of phosphorylated eIF2α are dramatically increased in accordance with the emergence of BACE1 elevation in 5XFAD mice at 8 months of age (Devi and Ohno, 2010b; Devi and Ohno, 2013a; Devi and Ohno, 2013b). Moreover, we demonstrated that increased amounts of phosphorylated eIF2α resulting from the application of Sal 003, a specific inhibitor of its phosphatase, can elevate BACE1 protein levels in 6-month-old 5XFAD mice (Devi and Ohno, 2010b). However, it remained unclear which eIF2α phosphorylation pathway would be responsible for mediating the elevation of BACE1 expression in AD. The eIF2α kinases except for HRI (predominantly found in erythroid cells) are prominently expressed in the mammalian brain (Costa-Mattioli and Sonenberg, 2008; Donnelly et al., 2013). In this study, we found that reducing PERK-dependent eIF2α phosphorylation blocks BACE1 elevation in advanced stages of 5XFAD mice (8–9-month-old), leading to the suppression of β-amyloidogenesis as evidenced by decreased levels of C99 fragments, Aβ40 and Aβ42 peptides, and amyloid plaque burden in PERK^{+/−}·5XFAD mice. In contrast, our previous investigations reveal that the PKR pathway is not activated even in old 5XFAD mice that have significantly elevated levels of phosphorylated eIF2α and BACE1 (Devi and Ohno, 2013a; Devi and Ohno, 2013b). Moreover, GCN2 gene deletion fails to block the eIF2α phosphorylation-associated upregulation of BACE1 in this AD model (Devi and Ohno, 2013a). Consistent with our observations in 5XFAD mice, transfection with dominant negative PERK, but not dominant negative GCN2, was reported to prevent energy deprivation-induced phosphorylation of eIF2α and BACE1 elevation *in vitro* (O'Connor et al., 2008). Therefore, the results demonstrate that overactivation of the PERK-eIF2α pathway may represent a crucial pathogenic mechanism underlying BACE1 elevation and consequent acceleration of neurotoxic Aβ/C99, at least, in the 5XFAD mouse model of AD.

Transgenic overexpression of multiple FAD mutant forms of human APP and PS1 is designed to trigger robust Aβ42 production in 5XFAD mice (Oakley et al., 2006). In the current study, we found that additional mechanisms, such as elevation in not only BACE1

but also full-length APP and reduction in the major Aβ-degrading enzyme neprilysin, are implicated in further accelerating the progression of amyloid pathology after Aβ accumulation reaches a certain level in this AD model (8–9 months of age). Interestingly, in addition to the complete reversal of BACE1 upregulation, we also observed that PERK haploinsufficiency partially but significantly lowers the expression of full-length APP in 5XFAD mice. The expression level of APP transgene in 5XFAD mice is under tight transcriptional control of the neuron-specific Thy-1 promoter. Therefore, the reduction in full-length APP protein in PERK$^{+/-}$·5XFAD mice relative to 5XFAD controls suggests that there is a posttranscriptional component of the APP overexpression in this model. Importantly, the changes in response to PERK haploinsufficiency are specific to 5XFAD mice, since levels of full-length APP as well as BACE1 are equivalent between PERK$^{+/-}$ and wild-type control mice. Moreover, our recent study reveals progressive increases of APP expression in 5XFAD mice with aging, which coincide with enhanced eIF2α phosphorylation (Devi and Ohno, unpublished data). Together, it seems reasonable to conceive that overactivation of the PERK-dependent eIF2α phosphorylation pathway in 5XFAD mice may be closely associated with the posttranscriptional elevation of APP, although further investigation is needed to understand the precise underlying mechanisms. This idea is also supported by our previous findings that not only BACE1 but also its substrate full-length APP is elevated concomitant with robust activation of the PERK-eIF2α pathway in younger (3- to 4-month-old) 5XFAD mice under insulin-deficient diabetic conditions or exposure to behavioral stress (Devi et al., 2010; Devi et al., 2012).

Meanwhile, PERK haploinsufficiency also restores reduced levels of neprilysin expression in 5XFAD mice. Similarly, Ma et al. (2013) report that conditional ablation of PERK in APP/PS1 transgenic mice also lowers cerebral Aβ concentrations concomitant with the correction of decreased neprilysin expression. However, in contrast to our results, neither BACE1 nor full-length APP levels are changed by PERK gene manipulation in their APP/PS1 mice. In this regard, it is important to note that BACE1 expression levels are not different between APP/PS1 and wild-type control mice, suggesting that PERK-dependent eIF2α phosphorylation in this model does not reach the level required to elicit BACE1 elevation. Therefore, the contradictory results concerning the mechanisms of Aβ reduction may be accounted for by the different lines of transgenic AD models used and/or neuropathological stages that represent a key determinant for the degree of overactivation of the PERK-eIF2α phosphorylation pathway. The current study, using the aggressive 5XFAD amyloid model that recapitulates BACE1 elevations as seen in human AD brains, indicates that suppressing the PERK-eIF2α signaling pathway can reduce Aβ accumulation through different mechanisms, including decreased Aβ generation (i.e., BACE1 and APP reductions) and rescued Aβ clearance (i.e., neprilysin elevation).

ATF4, a repressor of CREB (CREB2), is another signaling molecule of which translation is facilitated by eIF2α phosphorylation (Harding et al., 2000a; Vattem and Wek, 2004). Recent work demonstrates that genetic or pharmacologic stimulation of eIF2α phosphorylation impairs contextual memory consolidation through upregulation of ATF4 and consequent CREB dysfunction, whereas behavioral training for contextual conditioning results in reduced levels of phosphorylated eIF2α (Costa-Mattioli et al., 2007; Jiang et al., 2010). Furthermore, it has also been reported that genetic or pharmacologic suppression of eIF2α

phosphorylation reduces ATF4 levels and enhances memory performances on different learning tasks with weak training protocols (Costa-Mattioli et al., 2005; Costa-Mattioli et al., 2007; Stern et al., 2013). The neurobiological studies provide convergent evidence that eIF2α phosphorylation-dependent elevation of ATF4 negatively regulates memory consolidation processes through suppressing CREB activity. In accordance with this hypothesis, we demonstrate that 5XFAD mice suffering from memory decline recapitulate increased levels of ATF4 expression concomitant with robust elevations in phosphorylated eIF2α, as seen with AD brains (Lewerenz and Maher, 2009). More importantly, we found that both ATF4 elevation and CREB dysfunction are reversed in PERK$^{+/−}$·5XFAD mice that show improvements in contextual memory. Therefore, our findings indicate that PERK-mediated eIF2α phosphorylation may cause deficient CREB function through upregulation of the CREB repressor ATF4, leading to impairments of contextual memory consolidation in 5XFAD mice. However, it should be noted that there are multiple mechanisms for Aβ-dependent induction of CREB dysfunction such as impaired PKA and MAPK signaling pathways (Ma et al., 2007; Vitolo et al., 2002). Furthermore, recent evidence suggests that BACE1 may interact with adenylate cyclase and directly impair the PKA/CREB pathway independent of its β-secretase activity for Aβ production (Chen et al., 2012b). We cannot, therefore, rule out the possibility that reductions in BACE1 expression and/or Aβ concentrations found in PERK$^{+/−}$·5XFAD mice may also contribute to the rescue of CREB dysfunction.

Finally, the present study provides the first demonstration that PERK haploinsufficiency can prevent AD-like cholinergic neuron loss found in the medial septum of 5XFAD mice. Consistent with our observations, oral administration of the specific PERK inhibitor GSK2606414 is reported to prevent eIF2α phosphorylation and translational failure in prion-infected mice, leading to rescue from neurodegeneration, deficient synaptic proteins and clinical signs including memory impairments (Moreno et al., 2013). Therefore, these findings support the concept that the dysregulated PERK-eIF2α pathway may be a common molecular mechanism underlying neurodegeneration that occurs as a consequence of the accumulation of misfolded proteins.

In conclusion, the results presented here provide experimental evidence that PERK mediates overactivation of eIF2α phosphorylation responsible for multifaceted memory-deteriorating mechanisms associated with AD, such as acceleration of β-amyloidosis, CREB dysfunction, and cholinergic neurodegeneration. Notably, selective and orally bioavailable inhibitors of PERK have been recently developed for neurodegenerative disease therapy (Axten et al., 2012; Moreno et al., 2013), so it will be important to test, as a next step, whether treatments with these PERK inhibitors, including the regimen for timing and duration of drug administration during the progression of disease, can exert similar beneficial effects in relevant animal models of AD. Our gene-based findings warrant such preclinical evaluations of PERK inhibitor drugs as a novel disease-modifying therapeutic intervention to treat AD and related cognitive impairments.

Acknowledgments

References

Axten JM, Medina JR, Feng Y, Shu A, Romeril SP, Grant SW, Li WH, Heerding DA, Minthorn E, Mencken T, Atkins C, Liu Q, Rabindran S, Kumar R, Hong X, Goetz A, Stanley T, Taylor JD, Sigethy SD, Tomberlin GH, Hassell AM, Kahler KM, Shewchuk LM, Gampe RT. Discovery of 7-methyl-5-(1-{[3-(trifluoromethyl)phenyl]acetyl}-2,3-dihydro-1*H*-indol-5-yl)-7*H*-pyrrolo[2,3-d]pyrimidin-4-amine (GSK2606414), a potent and selective first-in-class inhibitor of protein kinase R (PKR)-like endoplasmic reticulum kinase (PERK). J Med Chem. 2012; 55:7193–7207. [PubMed: 22827572]

Cai Y, Zhang XM, Macklin LN, Cai H, Luo XG, Oddo S, Laferla FM, Struble RG, Rose GM, Patrylo PR, Yan XX. BACE1 elevation is involved in amyloid plaque development in the triple transgenic model of Alzheimer's disease: differential Aβ antibody labeling of early-onset axon terminal pathology. Neurotox Res. 2012; 21:160–174. [PubMed: 21725719]

Chang RC, Wong AK, Ng HK, Hugon J. Phosphorylation of eukaryotic initiation factor-2α (eIF2α) is associated with neuronal degeneration in Alzheimer's disease. Neuroreport. 2002; 13:2429–2432. [PubMed: 12499843]

Chen A, Muzzio IA, Malleret G, Bartsch D, Verbitsky M, Pavlidis P, Yonan AL, Vronskaya S, Grody MB, Cepeda I, Gilliam TC, Kandel ER. Inducible enhancement of memory storage and synaptic plasticity in transgenic mice expressing an inhibitor of ATF4 (CREB-2) and C/EBP proteins. Neuron. 2003; 39:655–669. [PubMed: 12925279]

Chen R, Zhang J, Wu Y, Wang D, Feng G, Tang YP, Teng Z, Chen C. Monoacylglycerol lipase is a therapeutic target for Alzheimer's disease. Cell Rep. 2012a; 2:1329–1339. [PubMed: 23122958]

Chen Y, Huang X, Zhang YW, Rockenstein E, Bu G, Golde TE, Masliah E, Xu H. Alzheimer's β-secretase (BACE1) regulates the cAMP/PKA/CREB pathway independently of β-amyloid. J Neurosci. 2012b; 32:11390–11395. [PubMed: 22895721]

Choi JH, Kaur G, Mazzella MJ, Morales-Corraliza J, Levy E, Mathews PM. Early endosomal abnormalities and cholinergic neuron degeneration in amyloid-β protein precursor transgenic mice. J Alzheimers Dis. 2013; 34:691–700. [PubMed: 23254640]

Costa-Mattioli M, Gobert D, Harding H, Herdy B, Azzi M, Bruno M, Bidinosti M, Ben Mamou C, Marcinkiewicz E, Yoshida M, Imataka H, Cuello AC, Seidah N, Sossin W, Lacaille JC, Ron D, Nader K, Sonenberg N. Translational control of hippocampal synaptic plasticity and memory by the eIF2α kinase GCN2. Nature. 2005; 436:1166–1173. [PubMed: 16121183]

Costa-Mattioli M, Gobert D, Stern E, Gamache K, Colina R, Cuello C, Sossin W, Kaufman R, Pelletier J, Rosenblum K, Krnjevic K, Lacaille JC, Nader K, Sonenberg N. eIF2α phosphorylation bidirectionally regulates the switch from short- to long-term synaptic plasticity and memory. Cell. 2007; 129:195–206. [PubMed: 17418795]

Costa-Mattioli M, Sonenberg N. Translational control of gene expression: a molecular switch for memory storage. Prog Brain Res. 2008; 169:81–95. [PubMed: 18394469]

De Pietri Tonelli D, Mihailovich M, Di Cesare A, Codazzi F, Grohovaz F, Zacchetti D. Translational regulation of BACE-1 expression in neuronal and non-neuronal cells. Nucleic Acids Res. 2004; 32:1808–1817. [PubMed: 15034149]

Devi L, Alldred MJ, Ginsberg SD, Ohno M. Sex- and brain region-specific acceleration of β-amyloidogenesis following behavioral stress in a mouse model of Alzheimer's disease. Mol Brain. 2010; 3:34. [PubMed: 21059265]

Devi L, Alldred MJ, Ginsberg SD, Ohno M. Mechanisms underlying insulin deficiency-induced acceleration of β-amyloidosis in a mouse model of Alzheimer's disease. PLoS One. 2012; 7:e32792. [PubMed: 22403710]

Devi L, Ohno M. Genetic reductions of β-site amyloid precursor protein-cleaving enzyme 1 and amyloid-β ameliorate impairment of conditioned taste aversion memory in 5XFAD Alzheimer's disease model mice. Eur J Neurosci. 2010a; 31:110–118. [PubMed: 20092558]

Devi L, Ohno M. Phospho-eIF2α level is important for determining abilities of BACE1 reduction to rescue cholinergic neurodegeneration and memory defects in 5XFAD mice. PLoS One. 2010b; 5:e12974. [PubMed: 20886088]

Devi L, Ohno M. 7,8-Dihydroxyflavone, a small-molecule TrkB agonist, reverses memory deficits and BACE1 elevation in a mouse model of Alzheimer's disease. Neuropsychopharmacology. 2012; 37:434–444. [PubMed: 21900882]

Devi L, Ohno M. Deletion of the eIF2α kinase GCN2 fails to rescue the memory decline associated with Alzheimer's disease. PLoS One. 2013a; 8:e77335. [PubMed: 24146979]

Devi L, Ohno M. Mechanisms that lessen benefits of β-secretase reduction in a mouse model of Alzheimer's disease. Transl Psychiatry. 2013b; 3:e284. [PubMed: 23880880]

Donnelly N, Gorman AM, Gupta S, Samali A. The eIF2α kinases: their structures and functions. Cell Mol Life Sci. 2013; 70:3493–3511. [PubMed: 23354059]

Fanselow MS. Contextual fear, gestalt memories, and the hippocampus. Behav Brain Res. 2000; 110:73–81. [PubMed: 10802305]

Franklin, KBJ.; Paxinos, G. The Mouse Brain in Stereotaxic Coordinates. 3. Academic Press; New York: 2008.

Fukumoto H, Cheung BS, Hyman BT, Irizarry MC. β-Secretase protein and activity are increased in the neocortex in Alzheimer disease. Arch Neurol. 2002; 59:1381–1389. [PubMed: 12223024]

Gale GD, Anagnostaras SG, Fanselow MS. Cholinergic modulation of pavlovian fear conditioning: effects of intrahippocampal scopolamine infusion. Hippocampus. 2001; 11:371–376. [PubMed: 11530841]

Harding HP, Novoa I, Zhang Y, Zeng H, Wek R, Schapira M, Ron D. Regulated translation initiation controls stress-induced gene expression in mammalian cells. Mol Cell. 2000a; 6:1099–1108. [PubMed: 11106749]

Harding HP, Zeng H, Zhang Y, Jungries R, Chung P, Plesken H, Sabatini DD, Ron D. Diabetes mellitus and exocrine pancreatic dysfunction in *perk–/–* mice reveals a role for translational control in secretory cell survival. Mol Cell. 2001; 7:1153–1163. [PubMed: 11430819]

Harding HP, Zhang Y, Bertolotti A, Zeng H, Ron D. *Perk* is essential for translational regulation and cell survival during the unfolded protein response. Mol Cell. 2000b; 5:897–904. [PubMed: 10882126]

Holsinger RM, McLean CA, Beyreuther K, Masters CL, Evin G. Increased expression of the amyloid precursor β-secretase in Alzheimer's disease. Ann Neurol. 2002; 51:783–786. [PubMed: 12112088]

Jawhar S, Trawicka A, Jenneckens C, Bayer TA, Wirths O. Motor deficits, neuron loss, and reduced anxiety coinciding with axonal degeneration and intraneuronal Aβ aggregation in the 5XFAD mouse model of Alzheimer's disease. Neurobiol Aging. 2012; 33:196.e129–196.e140. [PubMed: 20619937]

Jiang Z, Belforte JE, Lu Y, Yabe Y, Pickel J, Smith CB, Je HS, Lu B, Nakazawa K. eIF2α Phosphorylation-dependent translation in CA1 pyramidal cells impairs hippocampal memory consolidation without affecting general translation. J Neurosci. 2010; 30:2582–2594. [PubMed: 20164343]

Kim HS, Choi Y, Shin KY, Joo Y, Lee YK, Jung SY, Suh YH, Kim JH. Swedish amyloid precursor protein mutation increases phosphorylation of eIF2α in vitro and in vivo. J Neurosci Res. 2007; 85:1528–1537. [PubMed: 17393484]

Kimura R, Devi L, Ohno M. Partial reduction of BACE1 improves synaptic plasticity, recent and remote memories in Alzheimer's disease transgenic mice. J Neurochem. 2010; 113:248–261. [PubMed: 20089133]

Kimura R, Ohno M. Impairments in remote memory stabilization precede hippocampal synaptic and cognitive failures in 5XFAD Alzheimer mouse model. Neurobiol Dis. 2009; 33:229–235. [PubMed: 19026746]

Lammich S, Schobel S, Zimmer AK, Lichtenthaler SF, Haass C. Expression of the Alzheimer protease BACE1 is suppressed via its 5′-untranslated region. EMBO Rep. 2004; 5:620–625. [PubMed: 15167888]

Lewerenz J, Maher P. Basal levels of eIF2α phosphorylation determine cellular antioxidant status by regulating ATF4 and xCT expression. J Biol Chem. 2009; 284:1106–1115. [PubMed: 19017641]

Li R, Lindholm K, Yang LB, Yue X, Citron M, Yan R, Beach T, Sue L, Sabbagh M, Cai H, Wong P, Price D, Shen Y. Amyloid β peptide load is correlated with increased β-secretase activity in sporadic Alzheimer's disease patients. Proc Natl Acad Sci USA. 2004; 101:3632–3637. [PubMed: 14978286]

Ma QL, Harris-White ME, Ubeda OJ, Simmons M, Beech W, Lim GP, Teter B, Frautschy SA, Cole GM. Evidence of Aβ- and transgene-dependent defects in ERK-CREB signaling in Alzheimer's models. J Neurochem. 2007; 103:1594–1607. [PubMed: 17760871]

Ma T, Trinh MA, Wexler AJ, Bourbon C, Gatti E, Pierre P, Cavener DR, Klann E. Suppression of eIF2α kinases alleviates Alzheimer's disease-related plasticity and memory deficits. Nat Neurosci. 2013; 16:1299–1305. [PubMed: 23933749]

Maren S. Neurobiology of Pavlovian fear conditioning. Annu Rev Neurosci. 2001; 24:897–931. [PubMed: 11520922]

Mihailovich M, Thermann R, Grohovaz F, Hentze MW, Zacchetti D. Complex translational regulation of BACE1 involves upstream AUGs and stimulatory elements within the 5′ untranslated region. Nucleic Acids Res. 2007; 35:2975–2985. [PubMed: 17439957]

Moreno JA, Halliday M, Molloy C, Radford H, Verity N, Axten JM, Ortori CA, Willis AE, Fischer PM, Barrett DA, Mallucci GR. Oral treatment targeting the unfolded protein response prevents neurodegeneration and clinical disease in prion-infected mice. Sci Transl Med. 2013; 5:206ra138.

Moreno JA, Radford H, Peretti D, Steinert JR, Verity N, Martin MG, Halliday M, Morgan J, Dinsdale D, Ortori CA, Barrett DA, Tsaytler P, Bertolotti A, Willis AE, Bushell M, Mallucci GR. Sustained translational repression by eIFα-P mediates prion neurodegeneration. Nature. 2012; 485:507–511. [PubMed: 22622579]

Mouton-Liger F, Paquet C, Dumurgier J, Bouras C, Pradier L, Gray F, Hugon J. Oxidative stress increases BACE1 protein levels through activation of the PKR-eIF2α pathway. Biochim Biophys Acta. 2012; 1822:885–896. [PubMed: 22306812]

O'Connor T, Sadleir KR, Maus E, Velliquette RA, Zhao J, Cole SL, Eimer WA, Hitt B, Bembinster LA, Lammich S, Lichtenthaler SF, Hebert SS, De Strooper B, Haass C, Bennett DA, Vassar R. Phosphorylation of the translation initiation factor eIF2α increases BACE1 levels and promotes amyloidogenesis. Neuron. 2008; 60:988–1009. [PubMed: 19109907]

Oakley H, Cole SL, Logan S, Maus E, Shao P, Craft J, Guillozet-Bongaarts A, Ohno M, Disterhoft J, Van Eldik L, Berry R, Vassar R. Intraneuronal β-amyloid aggregates, neurodegeneration, and neuron loss in transgenic mice with five familial Alzheimer's disease mutations: potential factors in amyloid plaque formation. J Neurosci. 2006; 26:10129–10140. [PubMed: 17021169]

Ohno M. Failures to reconsolidate memory in a mouse model of Alzheimer's disease. Neurobiol Learn Mem. 2009; 92:455–459. [PubMed: 19435612]

Ohno M, Chang L, Tseng W, Oakley H, Citron M, Klein WL, Vassar R, Disterhoft JF. Temporal memory deficits in Alzheimer's mouse models: rescue by genetic deletion of BACE1. Eur J Neurosci. 2006; 23:251–260. [PubMed: 16420434]

Ohno M, Cole SL, Yasvoina M, Zhao J, Citron M, Berry R, Disterhoft JF, Vassar R. BACE1 gene deletion prevents neuron loss and memory deficits in 5XFAD APP/PS1 transgenic mice. Neurobiol Dis. 2007; 26:134–145. [PubMed: 17258906]

Ohno M, Frankland PW, Chen AP, Costa RM, Silva AJ. Inducible, pharmacogenetic approaches to the study of learning and memory. Nat Neurosci. 2001; 4:1238–1243. [PubMed: 11713472]

Page G, Rioux Bilan A, Ingrand S, Lafay-Chebassier C, Pain S, Perault Pochat MC, Bouras C, Bayer T, Hugon J. Activated double-stranded RNA-dependent protein kinase and neuronal death in models of Alzheimer's disease. Neuroscience. 2006; 139:1343–1354. [PubMed: 16581193]

Silva AJ, Kogan JH, Frankland PW, Kida S. CREB and memory. Annu Rev Neurosci. 1998; 21:127–148. [PubMed: 9530494]

Stern E, Chinnakkaruppan A, David O, Sonenberg N, Rosenblum K. Blocking the eIF2α kinase (PKR) enhances positive and negative forms of cortex-dependent taste memory. J Neurosci. 2013; 33:2517–2525. [PubMed: 23392680]

Trinh MA, Kaphzan H, Wek RC, Pierre P, Cavener DR, Klann E. Brain-specific disruption of the eIF2α kinase PERK decreases ATF4 expression and impairs behavioral flexibility. Cell Rep. 2012; 1:676–688. [PubMed: 22813743]

Vattem KM, Wek RC. Reinitiation involving upstream ORFs regulates ATF4 mRNA translation in mammalian cells. Proc Natl Acad Sci USA. 2004; 101:11269–11274. [PubMed: 15277680]

Vitolo OV, Sant'Angelo A, Costanzo V, Battaglia F, Arancio O, Shelanski M. Amyloid β-peptide inhibition of the PKA/CREB pathway and long-term potentiation: reversibility by drugs that enhance cAMP signaling. Proc Natl Acad Sci USA. 2002; 99:13217–13221. [PubMed: 12244210]

Wang S, Wang R, Chen L, Bennett DA, Dickson DW, Wang DS. Expression and functional profiling of neprilysin, insulin-degrading enzyme, and endothelin-converting enzyme in prospectively studied elderly and Alzheimer's brain. J Neurochem. 2010; 115:47–57. [PubMed: 20663017]

Yang LB, Lindholm K, Yan R, Citron M, Xia W, Yang XL, Beach T, Sue L, Wong P, Price D, Li R, Shen Y. Elevated β-secretase expression and enzymatic activity detected in sporadic Alzheimer disease. Nat Med. 2003; 9:3–4. [PubMed: 12514700]

Zhang P, McGrath B, Li S, Frank A, Zambito F, Reinert J, Gannon M, Ma K, McNaughton K, Cavener DR. The PERK eukaryotic initiation factor 2α kinase is required for the development of the skeletal system, postnatal growth, and the function and viability of the pancreas. Mol Cell Biol. 2002; 22:3864–3874. [PubMed: 11997520]

Zhao J, Fu Y, Yasvoina M, Shao P, Hitt B, O'Connor T, Logan S, Maus E, Citron M, Berry R, Binder L, Vassar R. β-Site amyloid precursor protein cleaving enzyme 1 levels become elevated in neurons around amyloid plaques: implications for Alzheimer's disease pathogenesis. J Neurosci. 2007; 27:3639–3649. [PubMed: 17409228]
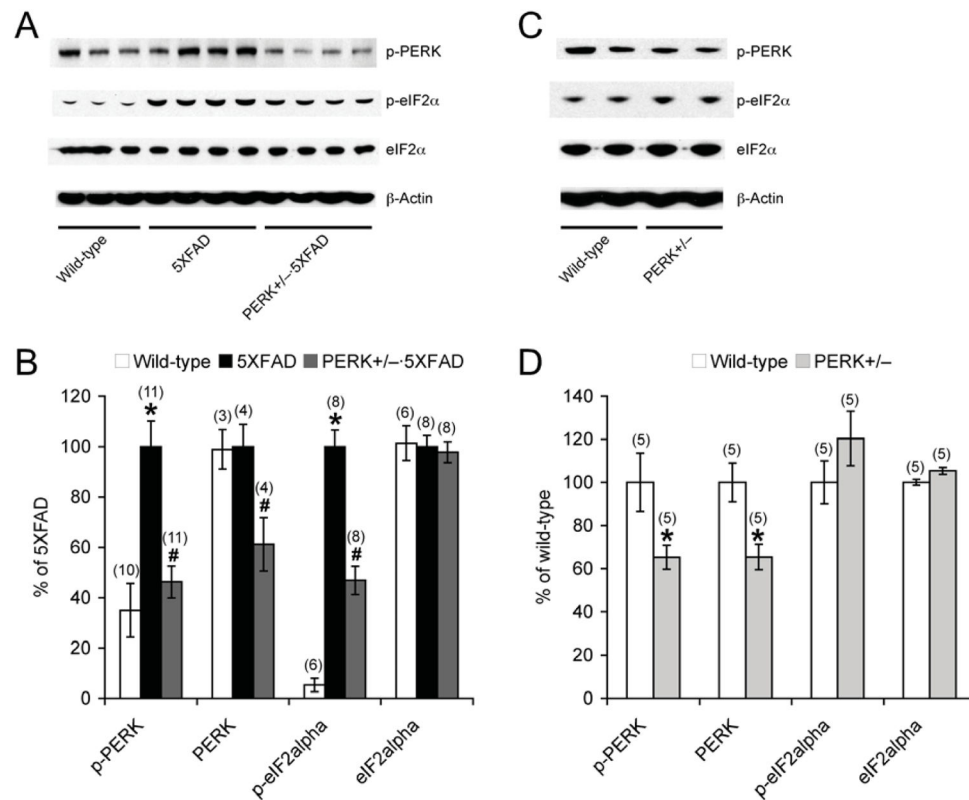
Fig. 1.
Effects of PERK haploinsufficiency on eIF2α phosphorylation in 5XFAD mice. (A, C)
Representative immunoblots of protein extracts from hippocampal homogenates of mice. (B,
D) Immunoreactive bands were quantified and expressed as the percentage of 5XFAD (B) or
wild-type control (D) mice. The number of animals used is indicated on top of each column.
Note that blocking PERK overactivation significantly suppressed increases in eIF2α
phosphorylation in 5XFAD mice without changes in total eIF2α levels. Meanwhile, levels
of phosphorylated eIF2α were indistinguishable between PERK^{+/−} and wild-type mice. All
data are presented as mean ± SEM and were analyzed by one-way ANOVA followed by
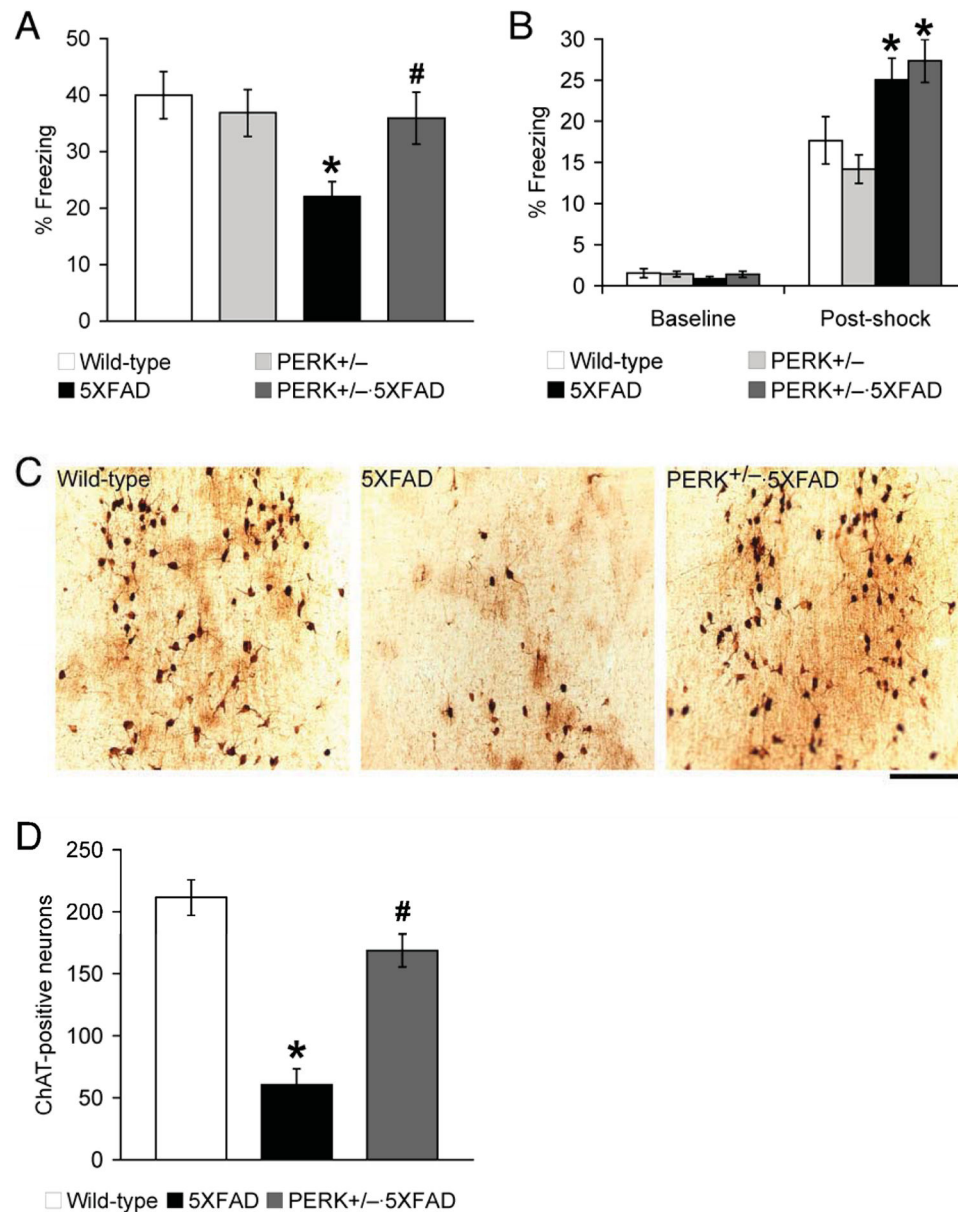*post-hoc* Fisher's PLSD test (* $p < 0.05$ vs. wild-type, [#] $p < 0.05$ vs. 5XFAD).

Fig. 2.

Effects of PERK haploinsufficiency on memory deficits and cholinergic neurodegeneration in 5XFAD mice. (A, B) Mice were trained with two CS-US pairings for contextual fear conditioning (wild-type, $n = 22$; PERK^{+/−}, $n = 24$; 5XFAD, $n = 28$; PERK^{+/−}·5XFAD, $n = 27$). Freezing behavior was assessed during training session (B) as well as 24-h memory retention test (A). 5XFAD mice showed significantly lower levels of contextual freezing than wild-type mice when tested 24 h after training. Note that PERK^{+/−}·5XFAD mice were rescued almost completely back to wild-type control levels of contextual memory. (C) Brain sections were immunostained for the cholinergic marker ChAT. Shown are representative photomicrographs of ChAT-immunoreactive neurons in the medial septum of mice. Scale bar = 200 μm. (D) The number of ChAT-positive neurons in the medial septum and the vertical limb of the diagonal band (Ch1/2), which provide the cholinergic innervation to the

hippocampus, was counted for quantification (wild-type, $n = 4$; 5XFAD, $n = 4$; PERK$^{+/-}$·5XFAD, $n = 5$). Note that PERK haploinsufficiency almost completely prevented cholinergic neurodegeneration in 5XFAD mice. All data are presented as mean ± SEM and were analyzed by one-way ANOVA followed by *post-hoc* Fisher's PLSD test (* $p < 0.05$ vs. wild-type, [#] $p < 0.05$ vs. 5XFAD).
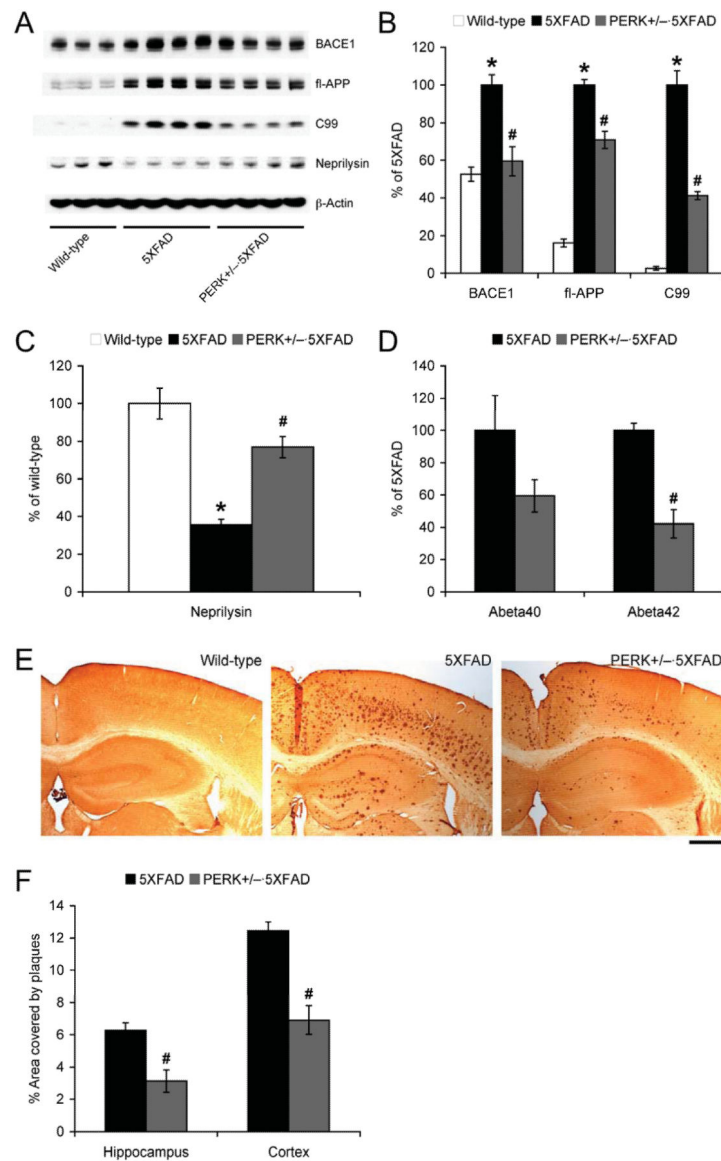
Fig. 3.

Effects of PERK haploinsufficiency on β-amyloidogenic processing of APP and Aβ accumulation in 5XFAD mice. (A) Representative immunoblots of protein extracts from hippocampal homogenates of mice. (B, C) Immunoreactive bands were quantified and expressed as the percentage of 5XFAD (B) or wild-type control (C) mice (wild-type, $n = 6$; 5XFAD, $n = 8$; PERK$^{+/-}$·5XFAD, $n = 8$). Note that PERK haploinsufficiency significantly reduced levels of BACE1, full-length APP and C99, while it restored decreased neprilysin expression in 5XFAD mice. (D) Levels of total Aβ40 and Aβ42 were quantified by sandwich ELISAs of guanidine extracts of hippocampal samples and expressed as the percentage of 5XFAD controls (5XFAD, $n = 9$; PERK$^{+/-}$·5XFAD, $n = 12$). (E) Brain sections were immunostained with the 6E10 anti-Aβ antibody. Shown are representative photomicrographs of the hippocampal and cortical regions. Scale bar = 500 μm. (F) Percentage area occupied by Aβ deposits in the hippocampus and cerebral cortex was

measured for quantification (5XFAD, $n = 7$; PERK$^{+/-}$·5XFAD, $n = 5$). PERK haploinsufficiency significantly reduced Aβ40 and Aβ42 concentrations as well as plaque burden in 5XFAD mice. All data are presented as mean ± SEM and were analyzed by one-way ANOVA followed by *post-hoc* Fisher's PLSD test (* $p < 0.05$ vs. wild-type, # $p < 0.05$ vs. 5XFAD).
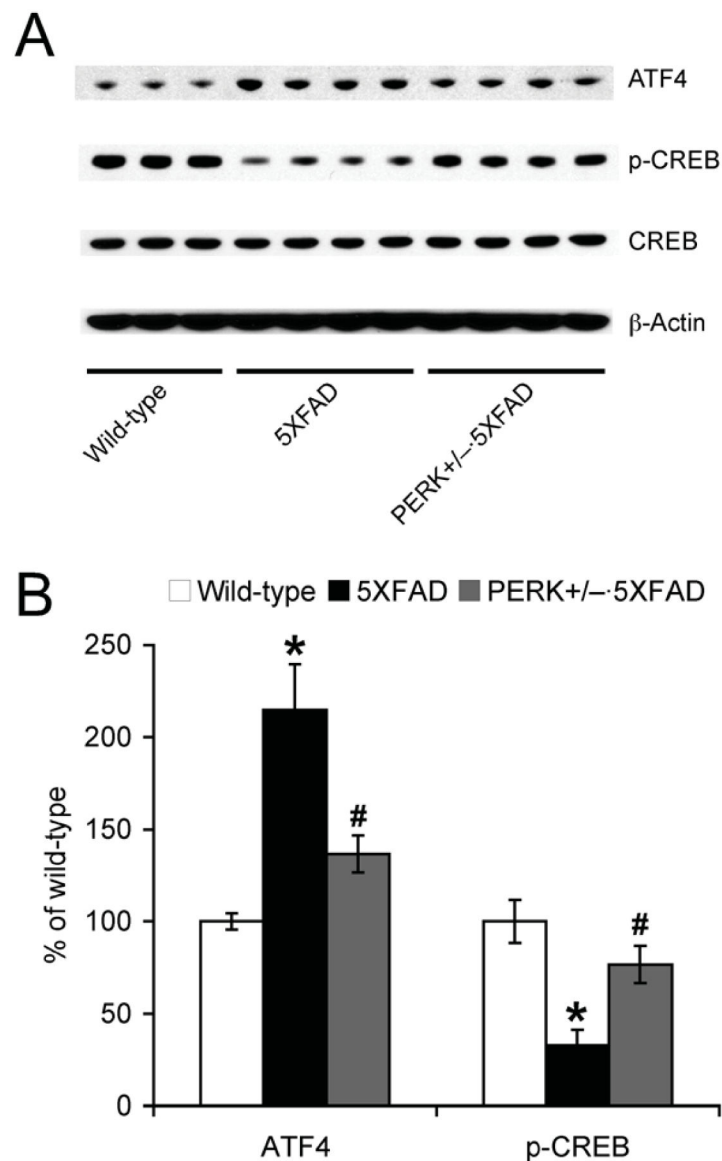
Fig. 4.
Effects of PERK haploinsufficiency on ATF4 and CREB pathways in 5XFAD mice. (A) Representative immunoblots of protein extracts from hippocampal homogenates of mice. (B) Immunoreactive bands were quantified and expressed as the percentage of wild-type control mice (wild-type, $n = 6$; 5XFAD, $n = 8$; PERK$^{+/-}$·5XFAD, $n = 8$). Note that PERK haploinsufficiency almost completely blocked ATF4 elevation, while it restored reduced levels of phosphorylated CREB without affecting total CREB in 5XFAD mice. All data are presented as mean ± SEM and were analyzed by one-way ANOVA followed by *post-hoc* Fisher's PLSD test (* $p < 0.05$ vs. wild-type, # $p < 0.05$ vs. 5XFAD).